

# VIDEO PANDA: VIDEO PANORAMIC DIFFUSION WITH MULTI-VIEW ATTENTION

Anonymous authors

Paper under double-blind review

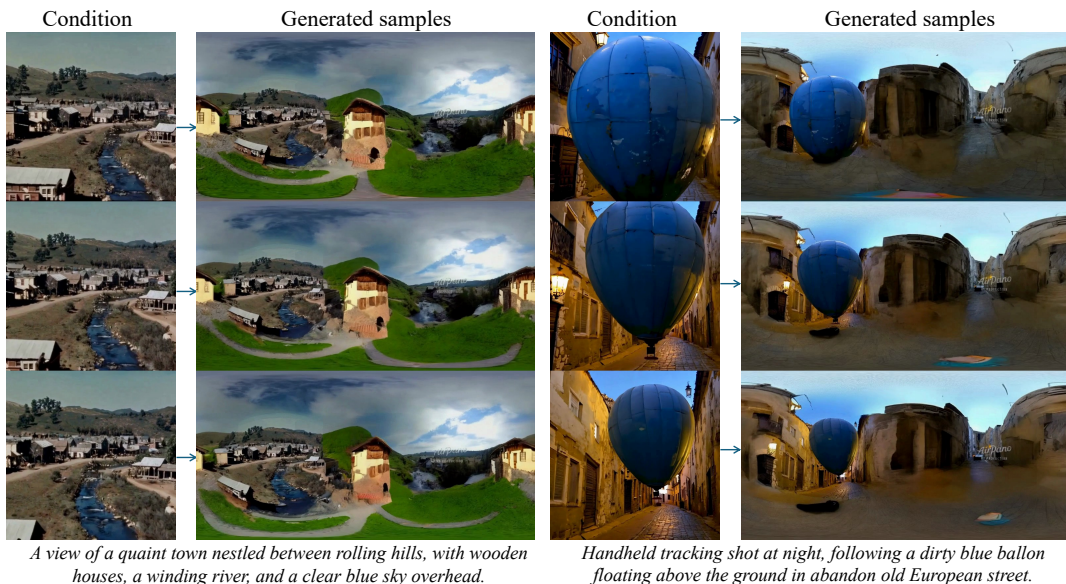


Figure 1: Generated samples conditioned on a single-view video and text prompt. Both single-view video inputs were generated using existing video generation models (Brooks et al., 2024; Runway, 2024). Autoregressive generation is applied to extend the video length.

## ABSTRACT

High resolution panoramic video content is paramount for immersive experiences in Virtual Reality, but is non-trivial to collect as it requires specialized equipment and intricate camera setups. In this work, we introduce VideoPanda, a novel approach for synthesizing 360° videos conditioned on text or single-view video data. VideoPanda leverages multi-view attention layers to augment a video diffusion model, enabling it to generate consistent multi-view videos that can be combined into immersive panoramic content. VideoPanda is trained jointly using two conditions: text-only and single-view video, and supports autoregressive generation of long-videos. To overcome the computational burden of multi-view video generation, we randomly subsample the duration and camera views used during training and show that the model is able to gracefully generalize to generating more frames during inference. Extensive evaluations on both real-world and synthetic video datasets demonstrate that VideoPanda generates more realistic and coherent 360° panoramas across all input conditions compared to existing methods. Visit the project website at <https://mvpanovideo.github.io/VideoPanda/> for results.

## 1 INTRODUCTION

A key aspect of achieving true immersion in a virtual environment is allowing users to look around freely, by rotating their head and exploring their surroundings from all possible angles. To en-

able such experiences, it is essential to have access to high-quality and high-resolution panoramic videos. However, recording such videos is both expensive and time-consuming, as it requires intricate camera setups and specialized equipment. As a result, the available panoramic video content on platforms such as YouTube or Vimeo remains limited compared to single-view videos. In this work, we aim to address this issue, by developing a generative model capable of synthesizing panoramic videos either from text prompts or by expanding single-view videos (either generated from models like Sora (Brooks et al., 2024) or recorded) into panoramic format. We consider this an essential step towards making immersive content more accessible and scalable.

Recently, diffusion models have shown remarkable success in generating images (Ho et al., 2022; Blattmann et al., 2023a), 3D models (Shi et al., 2023b; Poole et al., 2022), and videos (Brooks et al., 2024; Blattmann et al., 2023b) from text prompts. Despite their promising capabilities, generation of panoramic videos using diffusion models presents significant challenges, mainly due to the scarcity of high-quality panoramic video datasets. Furthermore, while substantial progress has been made towards advancing standard video generation pipelines (Girdhar et al., 2023; Hong et al., 2022; Chen et al., 2024; Zheng et al., 2024), very few works have attempted to apply these techniques to panoramic video generation. Existing methods are either limited to specific domains such as driving scenarios (Wen et al., 2024; Wu et al., 2024; Li et al., 2023; Zhao et al., 2024; Liu et al., 2024b) or restricted to generating static scenes (Wu et al., 2023; Zhang et al., 2024). 360DVD (Wang et al., 2024a) directly generates equirectangular panorama video (with text condition), which presents a large domain gap to base model pretrained on perspective view. We perform an extensive comparison to 360DVD in the text-conditional setting and demonstrate our improved visual quality.

In this paper, we introduce **VideoPanda**, a novel approach capable of generating high-quality panoramic videos from text prompts and single-view video, as well as creating long video using auto-regression. Our approach builds on existing video diffusion models by adding multi-view attention layers to generate consistent multi-view outputs. Doing so ensures that the output domain (perspective images) remains close to the original training distribution of the pretrained video model (as opposed to directly generating equirectangular projections), which helps in maintaining video quality while generating multiple views. The resulting views are then seamlessly stitched together to create a cohesive panoramic video. We evaluate our model on a diverse set of data domains, including both real and synthetic videos, and demonstrate its superior performance and quality compared to previous approaches, both quantitatively and qualitatively. Additionally, a user study indicates that the majority of participants prefer our generated videos over those from other baseline models. In summary, we make the following contributions:

- We identify the value of panoramic video generation by allowing users to input single-view videos as a condition – a widely available modality, and present a multi-view video architecture capable of generating plausible panoramic videos.
- We demonstrate that our model can be jointly trained for text-conditioning, video-conditioning, and autoregressive settings by randomizing the conditioning type, leading to improved results and enabling the generation of long panoramic videos.
- When extending the video model to multi-view, the number of generated image frames greatly increases. We overcome the inherent computational burden associated by randomly subselecting the number of views and frames and show that it gracefully generalizes to video with long duration and more views during inference.

## 2 RELATED WORK

### 2.1 IMAGE AND VIDEO DIFFUSION MODELS

Diffusion models (Ho et al., 2020) have demonstrated remarkable success in generating high-quality images (Karras et al., 2022; 2024; Pernias et al., 2023; Hoogeboom et al., 2023; Ho et al., 2022) and videos (Girdhar et al., 2023; Hong et al., 2022; Blattmann et al., 2023a;b; Brooks et al., 2024; Guo et al., 2023; Chen et al., 2023; Gupta et al., 2023) from text prompts. To reduce the computational cost of generating high-dimensional data such as images and videos, latent diffusion models (Rom-bach et al., 2022) (LDMs) proposed to first encode the data into a compressed latent space using a variational autoencoder (VAE) (Kingma, 2013a), and then conduct the diffusion in this lower dimensional space. These models have been proven highly effective for a wide range of downstream tasks

such as inpainting (Lugmayr et al., 2022), controllable generation (Zhang et al., 2023), customized generation (Ruiz et al., 2023), and image/video editing (Kawar et al., 2023; Molad et al., 2023) etc.

## 2.2 MULTI-VIEW IMAGE GENERATION

Building on the success of diffusion models for 2D image generation, they have been increasingly adapted also for multi-view image generation. However, due to the limited availability of real-world multi-view training data, several recent approaches (Shi et al., 2023b; Long et al., 2024; Liu et al., 2023b;a) attempted to fine-tune pretrained image generation models like Stable Diffusion (Rombach et al., 2022) to support multi-view generation. Such approaches can be roughly categorized into two categories: object-centric and scene-centric approaches.

Object-centric models focus primarily on generating images of objects where all cameras are inward-facing, looking at a single object from different viewing directions. Examples of such approaches include (Kant et al., 2024; Kong et al., 2024; Shi et al., 2023a;b; Tang et al., 2024; Voleti et al., 2024; Wang & Shi, 2023). More recently, several object-centric generative models explored incorporating custom attention mechanisms (Hu et al., 2024; Huang et al., 2023; Kant et al., 2024; Li et al., 2024b) to aggregate view-specific information across multiple views. Notable among these, CAT3D (Gao\* et al., 2024) trains a model that generates novel views of an inward-focused scene from one or more input views, allowing for 3D reconstruction from a single image. However, these methods often focus on single-object scenes, which limits their applicability to more complex environments.

The second line of work seeks to generate realistic multi-view images of entire scenes, using outward-facing cameras to capture different viewing directions and produce panoramas. For instance, PanoDiffusion (Wu et al., 2023) is trained on equirectangular projections of 360° panoramic images, and relies on inpainting during inference to extend the input images into complete panoramas. Building on this, PanFusion (Zhang et al., 2024) adds an additional branch to Stable Diffusion, enabling the simultaneous generation of panoramas and multi-view images. MVDiffusion (Tang et al., 2023) introduces correspondence-aware attention (CAA) layers, where each point attends only to other points within its local neighborhood. More recently (Yuan et al., 2024; Wang et al., 2023) proposed predicting the homography between input views and use a diffusion model to generate the unseen regions of the panorama. Lastly, LayerPano3D (Yang et al., 2024) combines multi-view and inpainting models to generate multi-layer panoramas, allowing for somewhat limited exploration within the scene boundaries. Other notable works in this area include (Li et al., 2024a; Zhou et al., 2024; Hara & Harada, 2024; Liu et al., 2024a).

## 2.3 MULTI-VIEW AND PANORAMA VIDEO GENERATION

The emergence of powerful open-source video diffusion models (Blattmann et al., 2023a; Chen et al., 2024; Zheng et al., 2024) gave rise to the development of several approaches aimed at augmenting them with multi-view capabilities (Watson et al., 2024) and extending them to generate 360° panoramic videos. For example, 360DVD (Wang et al., 2024a) builds upon a pretrained text-to-video model (Guo et al., 2023) by adding a 360-adaptor and fine-tuning it on equirectangular projections of panoramic videos. This enables the creation of 360° videos from a text inputs, with the option to condition on optical flow videos. Generative Camera Dolly (Van Hoorick et al., 2024) extends the image-conditional Stable Video Diffusion (Blattmann et al., 2023a) into a video-to-video model. Given an input video of a scene, (Blattmann et al., 2023a) can generate a synchronized video from a different camera trajectory. 4K4DGEN (Li et al., 2024c) draws inspiration from MultiDiffusion (Müller et al., 2024) and introduces a training-free method that denoises multiple views of a spherical panorama simultaneously. Most similar to our method is Panacea (Wen et al., 2024), which is inspired by VideoLDM (Blattmann et al., 2023a) and extends StableDiffusion by adding multi-view and temporal attention layers, trained on multi-view driving videos. Notably, Panacea relies on a dynamic birds’ eye view (BEV) representation as conditioning, which is most commonly available in the case of driving scenes, thus effectively limiting its applications to driving scenes.

## 3 METHOD

In this work, we introduce VideoPanda, a multi-view video diffusion model capable of generating long panoramic 360° videos from a text prompt or a perspective video. Below, we describe our

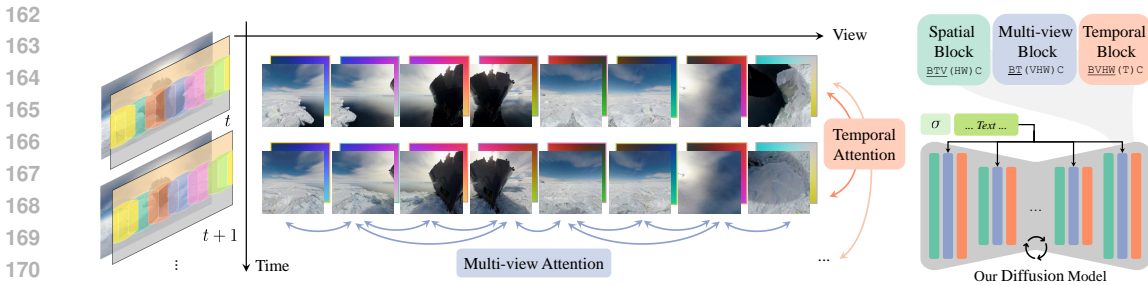


Figure 2: We divide the equi-rectangular video into 8 perspective views via projection. Our diffusion model consists of interleaved spatial, multi-view, and temporal blocks, conditioned on text prompts. Attention is used to propagate information through the multi-view videos to ensure consistency. The input views are embedded using the ray directions as visualized by the color map behind the perspective images.

multi-view video diffusion model (§ 3.1), detail the model training strategy (§ 3.2), and finally describe the approach for auto-regressively generating long videos (§ 3.3). Fig. 2 provides an overview of our general model design.

### 3.1 MODEL DESIGN

We train a multi-view video diffusion model that, given a text prompt and an optional set of conditioning frames, is able to jointly generate multiple multi-view consistent videos of different view directions that together cover a full 360° panoramic video.

Our architecture builds on video latent diffusion models (VLDM) (Blattmann et al., 2023b) by incorporating multi-view attention layers inspired by MVDream (Shi et al., 2023b) and injecting view direction embeddings into the model. Specifically, we add 3D multi-view self-attention layers that perform self-attention across images from different views at each frame of the video. These layers are combined with the existing 2D self-attention layers in a residual manner using zero-initialized convolutions, similar to ControlNets (Zhang et al., 2023). To provide the model with an understanding of viewing directions, we use ray direction representations that are the same height and width as the latent representations and encode the ray directions at each spatial location, following (Gao\* et al., 2024). These rays are defined relative to the camera pose of the first view, and are invariant to global 3D translations and rotations. The view embeddings are concatenated channel-wise with their corresponding latents and are fed into the model at the first layer using zero-initialized convolutions.

Given a set of target and optional conditioning frames of size  $512 \times 512 \times 3$ , each image is encoded into a latent representation of size  $64 \times 64 \times 4$  using a variational autoencoder (VAE) (Kingma, 2013b). To enable conditioning on specific frames, we adopt the approach from CAT3D (Gao\* et al., 2024). During training, the latents corresponding to the non-conditioned views are noised according to the diffusion process, while the latents of the conditioning frames are kept mostly clean. Following prior work (Ho et al., 2021), to improve robustness and prevent overfitting, we use **noise augmentation** by adding a small amount of noise  $\sigma$  to the input conditioning latents and pass this value  $\sigma$  to the model as well. A binary mask is concatenated channel-wise to distinguish between the input conditioning latents and the target frames to be predicted. The diffusion model is then trained to learn the joint distribution of these latent representations conditioned on the inputs. We incorporate classifier-free guidance (CFG) (Ho & Salimans, 2022) by randomly dropping the conditioning frames with a probability of 10% during training.

Finally, similar to prior works (Hoogeboom et al., 2023), we observe improved performance when shifting the noise schedule towards higher noise levels, as our model generates more image frames than the base video model. Please see Appendix A.2 for more details. We also find that using a  $v$ -prediction objective (Salimans & Ho, 2022) leads to more stable training compared to  $\epsilon$ -prediction, particularly with high-noise schedules.



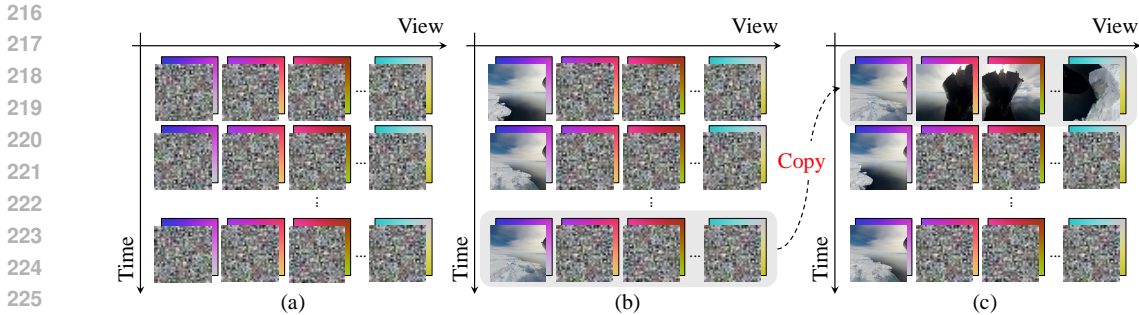


Figure 3: The model is trained using three frame conditioning regimes. (a) No image conditions and the initial inputs are pure noise; (b) Conditioning only on the first view of the video; (c) Conditioning on the first frame and first views for autoregressive video generation. At inference time, we autoregressively condition on long videos by using conditioning (b) to generate the first window and subsequently using the last multi-view images row from the previous time step (the shaded region) as the first row input to our model using condition-type (c).

### 3.2 TRAINING STRATEGY

We initialize the model from a pretrained text-to-video diffusion model (Blattmann et al., 2023b) which has been trained on web-scale video data. Following prior works (Shi et al., 2023b), the weights of the multi-view attention layers are initialized with the same weights as the existing 2D self-attention layers to accelerate training.

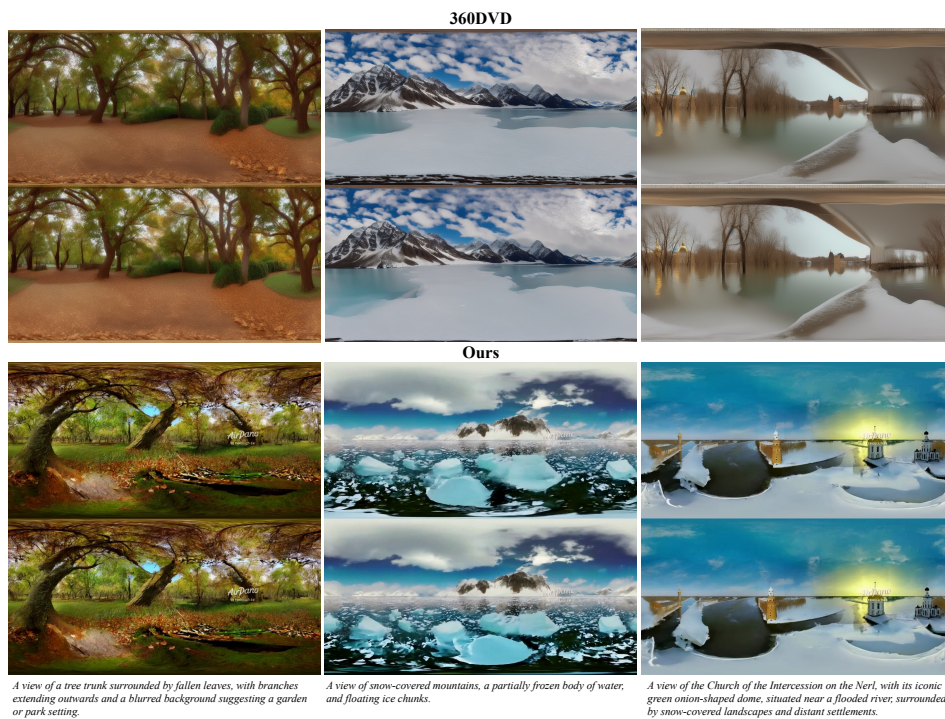
As we want to adjust the noise schedule (shifting toward higher noise levels) and change the model parametrization from  $\epsilon$ -prediction to  $v$ -prediction without overfitting the model to our limited panorama videos, we train our model in two stages. In the first stage, we finetune the single-view text-to-video model from the existing checkpoint, adapting it to the new noise schedule and loss objective. This stage is performed on a subset of the original pretraining data with standard captioned videos of 16 frames and requires minimal training time, as the model adapts quickly to these changes. In the second stage, we freeze the spatial layers of the video model and finetune the rest using multi-view video data.

During training, we randomize both the number of views and video frames to enhance the model’s generalization and prevent overfitting to the limited  $360^\circ$  video data, effectively using this as a form of data augmentation. The model is trained to generate multi-view video sequences represented as view-frame matrices of varying sizes, such as  $3 \times 16$ ,  $4 \times 12$ ,  $6 \times 8$ , and  $8 \times 6$ , where the first dimension refers to the number of views and the second to the number of frames. We refer to this randomization as **random matrix** going forward. This allows the model to generalize to new view-frame combinations, like  $8 \times 16$  matrices, during inference—configurations that couldn’t fit in GPU memory during training.

To handle multiple conditioning scenarios, we train a single general model that can generate multi-view videos conditioned on text, video, or a combination of video and the first frame’s multi-view images for autoregressive generation using a **multi-task** training strategy. Specifically, the binary mask is randomized to reflect these different conditioning setups: all zeros (text conditioning), the first column of ones with zeros elsewhere (video conditioning), or both the first row and first column set to ones (autoregressive generation), with equal probability. See Fig. 3 for a visualization of the different types of conditioning.

### 3.3 AUTOREGRESSIVE GENERATION OF LONG VIDEOS

To generate long panoramic videos, we use an autoregressive approach (see Fig. 3). Initially, conditioned on the first 16-frames of the input video, the model generates an  $8 \times 16$  view-frame matrix. For subsequent frames, the model is conditioned on the next 15 new frames of the video (a column) and the last frame from all 8 views (a row) generated in the previous step. This iterative process allows us to generate long, coherent video sequences with smooth transitions and consistent motion.



294 Figure 4: Qualitative figure compare text conditional video generation, 360DVD VS ours. The pixel  
295 quality of 360DVD is lower and distortion near the poles (top and bottom) is worse.

296  
297  
298 Autoregressive generation, however, tends to accumulate errors over time, leading to a gradual  
299 degradation in image quality and noticeable blurring after a few iterations. The noise augmen-  
300 tation introduced in § 3.1 helps mitigate this issue, consistent with findings from prior work (Valevski  
301 et al., 2024). This noise augmentation serves two purposes: it acts as a data augmentation technique  
302 to improve generalization, and it allows the model to self-correct by learning to recover clean infor-  
303 mation from noisy samples generated in previous iterations. Please see Appendix A.3 for details.

## 304 4 EXPERIMENTS

305  
306  
307 In this section, we explain the details of our experimental setting and our methodology for evalua-  
308 tions. We then present qualitative and quantitative comparisons to assess our models efficacy against  
309 baselines in text and video-conditional generation, demonstrate our models extension to long video  
310 generation and ablate key components of our training strategy. Additional training details are in-  
311 cluded in Appendix C.

### 312 4.1 DATA

313  
314 **Training Data.** We train our model on the WEB360 (Wang et al., 2024a) dataset, which contains  
315 2,114 panorama video clips with automatically generated captions. Each clip is 100 frames in length,  
316 totalling approximately 3 hours of footage that predominantly features panning shots of outdoor  
317 scenery.

318  
319 **Evaluation Data.** For the video conditioning task, we evaluate our method using two sources of  
320 data:

- 321 • In-distribution condition input: We gather 100 unseen panorama video clips from Youtube and  
322 extract 90 FOV horizontal perspective views for the input conditioning. Prompts are obtained by  
323 captioning the middle frame of the conditioning video using CogVLM (Wang et al., 2024b).

324  
325  
326  
327  
328  
329  
330  
331  
332  
333  
334  
335  
336  
337  
338  
339  
340  
341  
342  
343  
344  
345  
346  
347  
348  
349  
350  
351  
352  
353  
354  
355  
356  
357  
358  
359  
360  
361  
362  
363  
364  
365  
366  
367  
368  
369  
370  
371  
372  
373  
374  
375  
376  
377

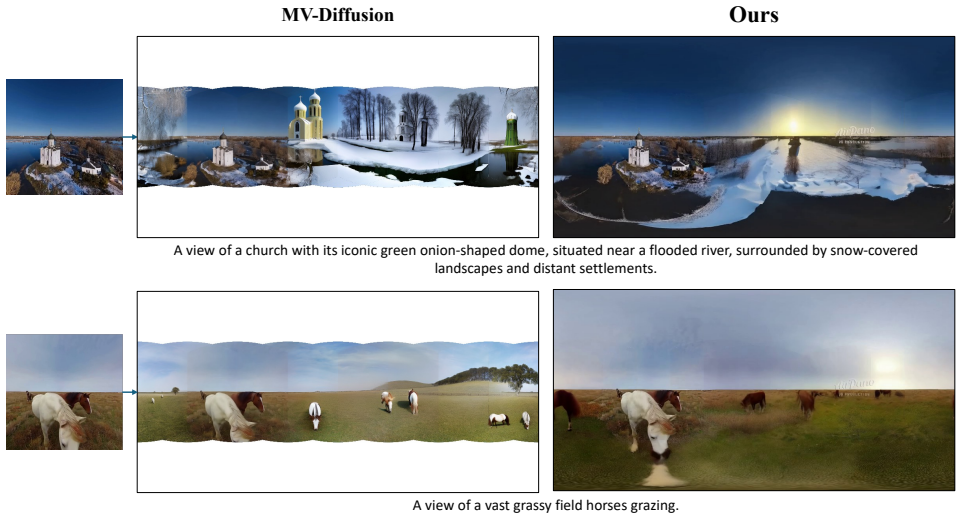


Figure 5: Qualitative figure comparing video conditional generation, MVDiffusion VS ours. Note that MVDiffusion can only outpace each frame of the video separately. MVDiffusion is worse at maintaining the structure and style of the input view globally compared to ours. For example the sky color and the scales and depths of objects is less consistent for MVDiffusion.

- Out-of-distribution condition input: We use generated videos from models including SORA (Brooks et al., 2024), Runway (Runway, 2024) and Luma (Lumalabs, 2024). These videos are cropped and resized to a resolution of  $512 \times 512$  and treated as horizontal side views. When available, we use the original prompt; otherwise, we caption the middle frame with CogVLM.

Since the out-of-distribution condition inputs do not originate from 360 videos, we cannot compute metrics that require ground truth images, such as pairwise FVD (Unterthiner et al., 2018) and the reconstruction metrics. Instead, we only evaluate them qualitatively. For the text conditional task, we use two data source: 100 prompts which are derived from captioning the in-distribution videos and 30 prompts generated by ChatGPT.

**Processing.** We first convert the equirectangular video data into multiple perspective views with overlap. A visualization is shown in Fig. 6. Similar to MVDiffusion we cover the horizontal side views with multiple perspective views of  $90^\circ$  FOV at  $0^\circ$  elevation. We empirically observed that the excessive amount of overlap stemming from the use of 8 horizontal views was unnecessary and thus we only use 6 views instead. These are evenly spaced in azimuth in offsets of  $60^\circ$ . We also explored using just 4 views which results in no overlaps between views similar to a cubemap representation but found that it was more difficult for the model to maintain consistency between views without overlaps. Additionally, to obtain a full panorama we add two perspective views looking straight up ( $90^\circ$  elevation) and down ( $-90^\circ$  elevation) to cover the ‘sky’ and ‘ground’ views. We increase the FOV for these two to  $100^\circ$  which is large enough to cover all pixels in the panorama when combined with the 6 side views.

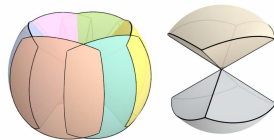


Figure 6: A visualization of the 8 frames used during training, consisting of 6 horizontal views with  $90^\circ$  FOV and 2 views for the top/bottom with  $100^\circ$  FOV

## 4.2 INFERENCE

Unless otherwise specified, we use a DDIM sampler with 25 steps and classifier-free guidance (CFG) to improve generation quality. In the text-conditional setting, we use a CFG scale of 8.0. For the video-conditional setting, we use a CFG scale of 4.0, where the unconditional score prediction does not take text nor video as input.

To facilitate fair evaluation, we use a common equirectangular format with resolution  $512 \times 1024$  for a 16 frame long panoramic video and compose our multi-view results into it by warping each of the images with bicubic interpolation. The pixel values in regions with overlap between views are uniformly averaged. When evaluating our generations, we either directly evaluate the stitched equirectangular video or following MVDiffusion, we crop 8 horizontal perspective view videos from it, since some metrics are more naturally evaluated using perspective views as input.

### 4.3 METRICS

**Validation Pair FID and FVD.** On validation sets we compare the set of generated frames to their paired real unseen frames in aggregate distribution. This evaluates both the quality and favors generations that adhere more closely to the true frames.

**Reconstruction Metrics.** In the video-conditional setting, we directly compare generated frames to their real counterparts as is commonly done for evaluating novel view synthesis performance. We use PSNR, SSIM and LPIPS (Zhang et al., 2018). Note that evaluating reconstruction metrics in the conditional generative setting can be problematic as the desired output is inherently ambiguous. Namely, direct comparisons with the ground truth can favor mode covering solutions, that may be lower in diversity.

**Clip Score (Clip).** We evaluate alignment to the supplied text prompt via clip score.

**User Preference.** We additionally conduct a user study, where equirectangular video/images from our model and the baseline are shown side-by-side to the user along with the conditioning input and they are asked to select their preferred result. For this setting, we randomly subsample 20 videos for each comparison and conducted the study with 6 users.

### 4.4 TEXT-CONDITIONAL GENERATION

We evaluate our model’s ability to generate multi-view videos from a text prompt and compare it to 360DVD (Wang et al., 2024a) that is our primary baseline. A quantitative comparison is summarized in Tab. 1. We note that our model outperforms 360DVD across all metrics. A side-by-side visual comparison is provided in Fig. 4, demonstrating that VideoPanda produces videos with higher image quality and sharper details. In contrast, 360DVD’s outputs extremely blurry and undersaturated results that suffer from insufficient warping near the top and bottom of the panoramas, hence leading to noticeable stretching artifacts when viewed in 3D, as we show in Appendix Fig. A5.

	Panorama			Horizontal 8 views			User Pref↑
	FID <sub>pair</sub> ↓	FVD <sub>pair</sub> ↓	Clip ↑	FID <sub>pair</sub> ↓	FVD <sub>pair</sub> ↓	Clip ↑	
360DVD	160	1942	28.4	128.7	958.2	27.6	28%
Ours (multi-task)	<b>136</b>	<b>1258</b>	<b>29.8</b>	<b>91.3</b>	<b>600.5</b>	<b>28.9</b>	<b>72%</b>

Table 1: Quantitative comparison for text-conditional panorama video generation.

### 4.5 VIDEO-CONDITIONAL GENERATION

Our video-conditional model accepts both a single view video and a text prompt which can be obtained through captioning the input view. During training, we randomly select one of the horizontal views, as shown in Fig. 6, as the conditional one and do not apply any noise on it. We exclude conditioning on top and bottom views as this case is less common. During inference we directly treat the input video as one of our horizontal views.

For general videos, there are no existing models that consider the video-conditional panoramic video generation task. Therefore, we compare our model to existing image-conditional panorama image generation model, MVDiffusion, at the frame level. In particular, for our method, we first generate a 16 frame panoramic video and then extract the middle frame. We compare against the outpainting model from MVDiffusion and report the results in Tab. 2. Since MVDiffusion does not cover the sky or ground regions, we only evaluate metrics on the 8 horizontal views. Our method scores significantly better on FID and reconstruction metrics, while being slightly worse on the clip score. Qualitatively we find that our method is much better at maintaining the style and scene scale/depth



	Horizontal 8 views					User Pref↑
	FID ↓	Clip ↑	PSNR ↑	LPIPS ↓	SSIM ↑	
MVDiffusion	96.8	<b>29.7</b>	13.4	0.568	0.485	23%
Ours (multi-task)	<b>63.2</b>	28.5	<b>17.6</b>	<b>0.457</b>	<b>0.636</b>	<b>77%</b>

Table 2: Quantitative comparison of single view video-conditional panorama generation with image panorama outpainting method MVDiffusion. We extract the middle frame from our 16 frame generations to compare at a per image level.

Ours Ablation		Panorama				Horizontal 8 view videos			
multi-task	rand-mat	FID↓	FVD↓	Clip ↑	PSNR ↑	FID ↓	FVD ↓	Clip ↑	PSNR ↑
✓	✓	<b>98</b>	916	<b>29.6</b>	15.9	49.8	258	<b>28.6</b>	17.6
×	✓	103	<b>861</b>	28.9	16.0	<b>48.4</b>	<b>255</b>	28.2	17.3
×	×	124	999	27.1	<b>17.0</b>	69.8	445	26.0	<b>18.5</b>

Table 3: Quantitative ablations of our model on single view video-conditional panoramic video generation. Training our model to be multi-task capable incurs a negligible drop in performance. Randomizing the matrix of frames during training results in much improved video quality at a slightly worse color consistency as measured by PSNR.

in the other generated views as demonstrated in the qualitative examples from Fig. 5. We also tried comparing to PanoDiffusion but found that this model is prone to over-fitting to indoor room scenes. We additionally, perform video-conditional generation on out of distribution videos and show generated results in Fig. 1 and our project website.

#### 4.6 AUTOREGRESSIVE GENERATION

To demonstrate our model’s performance on long video generation, we run 4 iterations of autoregression, resulting in a total of  $4 \times 15 + 1 = 61$  frames for the panorama videos. We observe that, despite using noise augmentation, autoregressive errors gradually accumulate, causing the scene to become blurry. To mitigate this, the noise-augmentation value can be increased during inference to regenerate finer details, though this introduces slight flickering due to the newly added details. Ideally, a dynamic system could be developed to increase the value when blurriness occurs and reduce it otherwise, minimizing flickering while keeping pixel quality high—an avenue we leave for future work. We provide examples of extracted frames from our autoregressively generated videos in Fig. 1 and Fig. B1. Please see our website for best viewing of long video generations.

#### 4.7 ABLATIONS

We ablate the main components of our method and include additional ablations on shifting the noise schedule of the base model, the architecture for conditioning on image frames and noise augmentation in Appendix A.

**Random Matrix vs. Fixed Matrix.** During training, we can fit a maximum of 6 time frames with 8 multi-views in memory. However, at inference we wish to generate 16 frames which is the native frame length for our base video model and aligns with 360DVD. To enable this we employ the randomized matrix strategy described in § 3.3. To evaluate the benefit of this strategy, we compare  $8 \times 16$  video-conditional generations from a model that was trained with the “random-matrix” strategy using an even mix of  $8 \times 6$ ,  $4 \times 12$  and  $3 \times 16$  with one using a “fixed-matrix” strategy trained with only the  $8 \times 6$  setting. We include a quantitative comparison in Tab. 3 and qualitative examples in Fig. 7. From the comparison, we see that the fixed-matrix trained model can create more blurry regions in its generations which is also reflected in significantly higher FID and FVD and somewhat lower clip score. Reconstruction metrics are very similar but slightly prefer the fixed-matrix model. We hypothesize that focusing training more on the 8 view case could slightly improve the global color consistency at the cost of worse visual quality.



496 Figure 7: Qualitative figure comparing full matrix and random matrix training. Random matrix  
497 training generates more high frequency details.



505 Figure 8: Qualitative figure comparing our single task vs multi-task model both generating 6 views  
506 on out of distribution video. Multi-task training provides better pixel quality. Moreover, with multi-  
507 task training, we can train one unified model for different tasks including video conditional genera-  
508 tion and auto-regressive generation.

509  
510  
511 **Multi-task Training.** We find that we can train one unified model to handle text-only conditioning,  
512 single view video conditioning and autoregressive conditioning. In Tab. 3 we also quantitatively  
513 compare our multi-task model with one only trained for the video conditional setting. For all the  
514 metrics, the multi-task model is marginally worse but very close indicating that we can train our  
515 model jointly with negligible impact to the quality. We also observe on some OOD conditions, that  
516 the random conditioned model tends to improve pixel quality slightly as seen in Fig. 8 which could  
517 be due to better generalization from multi-task training.

## 518 519 5 CONCLUSION

520  
521 We present VideoPanda, a model for panoramaic video generation. VideoPanda augments a pre-  
522 trained video diffusion model with the ability to generate consistent multiview videos that together  
523 cover a full panoramic video. We train VideoPanda in a unified manner with flexible conditioning  
524 supporting text and single-view video-conditioning and further support auto-regressive generation  
525 of longer videos.

526 Although VideoPanda demonstrates compelling results, there is still room for further improvement.  
527 The generation capabilities of our model are restricted by the performance of the base video model  
528 and further improvements could be obtained by applying these techniques to more powerful video  
529 diffusion models. Our model currently requires the field of view and elevation of the conditioning  
530 input to be sufficiently close to the configuration used in training. This could be addressed by  
531 estimating these parameters as demonstrated by recent work in the image generation domain (Yuan  
532 et al., 2024). Our autoregressive generation balances a trade-off between maintaining image qual-  
533 ity over time and consistency between windows which motivates investigating methods that could  
534 efficiently achieve both.

## 535 536 REFERENCES

537  
538 Andreas Blattmann, Tim Dockhorn, Sumith Kulal, Daniel Mendelevitch, Maciej Kilian, Dominik  
539 Lorenz, Yam Levi, Zion English, Vikram Voleti, Adam Letts, et al. Stable video diffusion: Scaling  
latent video diffusion models to large datasets. *arXiv preprint arXiv:2311.15127*, 2023a.

- 540 Andreas Blattmann, Robin Rombach, Huan Ling, Tim Dockhorn, Seung Wook Kim, Sanja Fidler,  
541 and Karsten Kreis. Align your latents: High-resolution video synthesis with latent diffusion  
542 models. In *IEEE Conference on Computer Vision and Pattern Recognition (CVPR)*, 2023b.
- 543
- 544 Tim Brooks, Bill Peebles, Connor Holmes, Will DePue, Yufei Guo, Li Jing, David Schnurr, Joe  
545 Taylor, Troy Luhman, Eric Luhman, Clarence Ng, Ricky Wang, and Aditya Ramesh. Video  
546 generation models as world simulators. 2024. URL [https://openai.com/research/  
547 video-generation-models-as-world-simulators](https://openai.com/research/video-generation-models-as-world-simulators).
- 548 Haoxin Chen, Yong Zhang, Xiaodong Cun, Menghan Xia, Xintao Wang, Chao Weng, and Ying  
549 Shan. Videocrafter2: Overcoming data limitations for high-quality video diffusion models, 2024.
- 550
- 551 Shoufa Chen, Mengmeng Xu, Jiawei Ren, Yuren Cong, Sen He, Yanping Xie, Animesh Sinha, Ping  
552 Luo, Tao Xiang, and Juan-Manuel Perez-Rua. Gentrion: Delving deep into diffusion transformers  
553 for image and video generation. *arXiv preprint arXiv:2312.04557*, 2023.
- 554 Ruiqi Gao\*, Aleksander Holynski\*, Philipp Henzler, Arthur Brussee, Ricardo Martin-Brualla,  
555 Pratul P. Srinivasan, Jonathan T. Barron, and Ben Poole\*. Cat3d: Create anything in 3d with  
556 multi-view diffusion models. *arXiv*, 2024.
- 557
- 558 Rohit Girdhar, Mannat Singh, Andrew Brown, Quentin Duval, Samaneh Azadi, Sai Saketh Ramb-  
559 hatla, Akbar Shah, Xi Yin, Devi Parikh, and Ishan Misra. Emu video: Factorizing text-to-video  
560 generation by explicit image conditioning. *arXiv preprint arXiv:2311.10709*, 2023.
- 561 Yuwei Guo, Ceyuan Yang, Anyi Rao, Zhengyang Liang, Yaohui Wang, Yu Qiao, Maneesh  
562 Agrawala, Dahua Lin, and Bo Dai. Animatediff: Animate your personalized text-to-image diffu-  
563 sion models without specific tuning. *arXiv preprint arXiv:2307.04725*, 2023.
- 564
- 565 Agrim Gupta, Lijun Yu, Kihyuk Sohn, Xiuye Gu, Meera Hahn, Li Fei-Fei, Irfan Essa, Lu Jiang,  
566 and José Lezama. Photorealistic video generation with diffusion models. *arXiv preprint  
567 arXiv:2312.06662*, 2023.
- 568 Takayuki Hara and Tatsuya Harada. Magritte: Manipulative and generative 3d realization from  
569 image, topview and text. *arXiv preprint arXiv:2404.00345*, 2024.
- 570
- 571 Jonathan Ho and Tim Salimans. Classifier-free diffusion guidance. *arXiv preprint  
572 arXiv:2207.12598*, 2022.
- 573
- 574 Jonathan Ho, Ajay Jain, and Pieter Abbeel. Denoising diffusion probabilistic models. *Advances in  
575 neural information processing systems*, 33:6840–6851, 2020.
- 576 Jonathan Ho, Chitwan Saharia, William Chan, David J Fleet, Mohammad Norouzi, and Tim  
577 Salimans. Cascaded diffusion models for high fidelity image generation. *arXiv preprint  
578 arXiv:2106.15282*, 2021.
- 579
- 580 Jonathan Ho, William Chan, Chitwan Saharia, Jay Whang, Ruiqi Gao, Alexey Gritsenko, Diederik P  
581 Kingma, Ben Poole, Mohammad Norouzi, David J Fleet, et al. Imagen video: High definition  
582 video generation with diffusion models. *arXiv preprint arXiv:2210.02303*, 2022.
- 583 Wenyi Hong, Ming Ding, Wendi Zheng, Xinghan Liu, and Jie Tang. Cogvideo: Large-scale pre-  
584 training for text-to-video generation via transformers. *arXiv preprint arXiv:2205.15868*, 2022.
- 585
- 586 Emiel Hooeboom, Jonathan Heek, and Tim Salimans. simple diffusion: End-to-end diffusion for  
587 high resolution images. In *International Conference on Machine Learning*, 2023. URL [https://  
588 //api.semanticscholar.org/CorpusID:256274516](https://api.semanticscholar.org/CorpusID:256274516).
- 589 Hanzhe Hu, Zhizhuo Zhou, Varun Jampani, and Shubham Tulsiani. Mvd-fusion: Single-view 3d via  
590 depth-consistent multi-view generation. In *CVPR*, 2024.
- 591
- 592 Zehuan Huang, Hao Wen, Junting Dong, Yaohui Wang, Yangguang Li, Xinyuan Chen, Yan-Pei  
593 Cao, Ding Liang, Yu Qiao, Bo Dai, et al. Epidiff: Enhancing multi-view synthesis via localized  
epipolar-constrained diffusion. *arXiv preprint arXiv:2312.06725*, 2023.

- 594 Yash Kant, Aliaksandr Siarohin, Ziyi Wu, Michael Vasilkovsky, Guocheng Qian, Jian Ren, Riza Alp  
595 Guler, Bernard Ghanem, Sergey Tulyakov, and Igor Gilitschenski. Spad: Spatially aware multi-  
596 view diffusers. In *Proceedings of the IEEE/CVF Conference on Computer Vision and Pattern  
597 Recognition*, pp. 10026–10038, 2024.
- 598 Tero Karras, Miika Aittala, Timo Aila, and Samuli Laine. Elucidating the design space of diffusion-  
599 based generative models. In *Proc. NeurIPS*, 2022.
- 601 Tero Karras, Miika Aittala, Jaakko Lehtinen, Janne Hellsten, Timo Aila, and Samuli Laine. Analyz-  
602 ing and improving the training dynamics of diffusion models. In *Proc. CVPR*, 2024.
- 603 Bahjat Kawar, Shiran Zada, Oran Lang, Omer Tov, Huiwen Chang, Tali Dekel, Inbar Mosseri, and  
604 Michal Irani. Imagic: Text-based real image editing with diffusion models. In *Proceedings of the  
605 IEEE/CVF Conference on Computer Vision and Pattern Recognition*, pp. 6007–6017, 2023.
- 607 Diederik P Kingma. Auto-encoding variational bayes. *arXiv preprint arXiv:1312.6114*, 2013a.
- 608 Diederik P Kingma. Auto-encoding variational bayes. *arXiv preprint arXiv:1312.6114*, 2013b.
- 609 Xin Kong, Shikun Liu, Xiaoyang Lyu, Marwan Taher, Xiaojuan Qi, and Andrew J Davison. Esch-  
610 ernet: A generative model for scalable view synthesis. *arXiv preprint arXiv:2402.03908*, 2024.
- 611 Ming-Feng Li, Yueh-Feng Ku, Hong-Xuan Yen, Chi Liu, Yu-Lun Liu, Albert Chen, Cheng-Hao  
612 Kuo, and Min Sun. Genrc: Generative 3d room completion from sparse image collections. 2024a.
- 613 Peng Li, Yuan Liu, Xiaoxiao Long, Feihu Zhang, Cheng Lin, Mengfei Li, Xingqun Qi, Shanghang  
614 Zhang, Wenhan Luo, Ping Tan, et al. Era3d: High-resolution multiview diffusion using efficient  
615 row-wise attention. *arXiv preprint arXiv:2405.11616*, 2024b.
- 616 Renjie Li, Panwang Pan, Bangbang Yang, Dejie Xu, Shijie Zhou, Xuanyang Zhang, Zeming Li,  
617 Achuta Kadambi, Zhangyang Wang, and Zhiwen Fan. 4k4dgen: Panoramic 4d generation at 4k  
618 resolution. *ArXiv*, abs/2406.13527, 2024c. URL [https://api.semanticscholar.org/  
619 CorpusID:270619480](https://api.semanticscholar.org/CorpusID:270619480).
- 620 Xiaofan Li, Yifu Zhang, and Xiaoqing Ye. Drivingdiffusion: Layout-guided multi-view driving  
621 scene video generation with latent diffusion model. *arXiv preprint arXiv:2310.07771*, 2023.
- 622 Aoming Liu, Zhong Li, Zhang Chen, Nannan Li, Yi Xu, and Bryan A Plummer. Panofree:  
623 Tuning-free holistic multi-view image generation with cross-view self-guidance. *arXiv preprint  
624 arXiv:2408.02157*, 2024a.
- 625 Buyu Liu, Kai Wang, Yansong Liu, Jun Bao, Tingting Han, and Jun Yu. Mvpbev: Multi-view  
626 perspective image generation from bev with test-time controllability and generalizability. *arXiv  
627 preprint arXiv:2407.19468*, 2024b.
- 628 Ruoshi Liu, Rundi Wu, Basile Van Hoorick, Pavel Tokmakov, Sergey Zakharov, and Carl Vondrick.  
629 Zero-1-to-3: Zero-shot one image to 3d object. In *Proceedings of the IEEE/CVF international  
630 conference on computer vision*, pp. 9298–9309, 2023a.
- 631 Yuan Liu, Cheng Lin, Zijiao Zeng, Xiaoxiao Long, Lingjie Liu, Taku Komura, and Wenping Wang.  
632 Syncdreamer: Generating multiview-consistent images from a single-view image. *arXiv preprint  
633 arXiv:2309.03453*, 2023b.
- 634 Xiaoxiao Long, Yuan-Chen Guo, Cheng Lin, Yuan Liu, Zhiyang Dou, Lingjie Liu, Yuexin Ma,  
635 Song-Hai Zhang, Marc Habermann, Christian Theobalt, et al. Wonder3d: Single image to 3d  
636 using cross-domain diffusion. In *Proceedings of the IEEE/CVF Conference on Computer Vision  
637 and Pattern Recognition*, pp. 9970–9980, 2024.
- 638 Andreas Lugmayr, Martin Danelljan, Andres Romero, Fisher Yu, Radu Timofte, and Luc Van Gool.  
639 Repaint: Inpainting using denoising diffusion probabilistic models. In *Proceedings of the  
640 IEEE/CVF conference on computer vision and pattern recognition*, pp. 11461–11471, 2022.
- 641 Lumalabs. Dream machine., 2024. URL <https://lumalabs.ai/dream-machine>.



- 648 Eyal Molad, Eliahu Horwitz, Dani Valevski, Alex Rav Acha, Yossi Matias, Yael Pritch, Yaniv  
649 Leviathan, and Yedid Hoshen. Dreamix: Video diffusion models are general video editors. *arXiv*  
650 *preprint arXiv:2302.01329*, 2023.
- 651 Norman Müller, Katja Schwarz, Barbara Rössle, Lorenzo Porzi, Samuel Rota Bulò, Matthias  
652 Nießner, and Peter Kotschieder. Multidiff: Consistent novel view synthesis from a single image.  
653 In *Proceedings of the IEEE/CVF Conference on Computer Vision and Pattern Recognition*, pp.  
654 10258–10268, 2024.
- 655 Pablo Pernias, Dominic Rampas, Mats L Richter, Christopher J Pal, and Marc Aubreville.  
656 Würstchen: An efficient architecture for large-scale text-to-image diffusion models. *arXiv*  
657 *preprint arXiv:2306.00637*, 2023.
- 658 Ben Poole, Ajay Jain, Jonathan T. Barron, and Ben Mildenhall. Dreamfusion: Text-to-3d using 2d  
659 diffusion. *arXiv*, 2022.
- 660 Robin Rombach, Andreas Blattmann, Dominik Lorenz, Patrick Esser, and Björn Ommer. High-  
661 resolution image synthesis with latent diffusion models. In *Proceedings of the IEEE/CVF confer-*  
662 *ence on computer vision and pattern recognition*, pp. 10684–10695, 2022.
- 663 Nataniel Ruiz, Yuanzhen Li, Varun Jampani, Yael Pritch, Michael Rubinstein, and Kfir Aberman.  
664 Dreambooth: Fine tuning text-to-image diffusion models for subject-driven generation. In *Pro-*  
665 *ceedings of the IEEE/CVF conference on computer vision and pattern recognition*, pp. 22500–  
666 22510, 2023.
- 667 Runway. Tools for human imagination., 2024. URL <https://runwayml.com/product>.
- 668 Tim Salimans and Jonathan Ho. Progressive distillation for fast sampling of diffusion models, 2022.  
669 URL <https://arxiv.org/abs/2202.00512>.
- 670 Ruoxi Shi, Hansheng Chen, Zhuoyang Zhang, Minghua Liu, Chao Xu, Xinyue Wei, Linghao Chen,  
671 Chong Zeng, and Hao Su. Zero123++: a single image to consistent multi-view diffusion base  
672 model. *arXiv preprint arXiv:2310.15110*, 2023a.
- 673 Yichun Shi, Peng Wang, Jianglong Ye, Long Mai, Kejie Li, and Xiao Yang. Mvdream: Multi-view  
674 diffusion for 3d generation. *arXiv:2308.16512*, 2023b.
- 675 Shitao Tang, Fuyang Zhang, Jiacheng Chen, Peng Wang, and Yasutaka Furukawa. Mvdiffusion:  
676 Enabling holistic multi-view image generation with correspondence-aware diffusion. *arXiv*, 2023.
- 677 Shitao Tang, Jiacheng Chen, Dilin Wang, Chengzhou Tang, Fuyang Zhang, Yuchen Fan, Vikas  
678 Chandra, Yasutaka Furukawa, and Rakesh Ranjan. Mvdiffusion++: A dense high-resolution  
679 multi-view diffusion model for single or sparse-view 3d object reconstruction. *arXiv preprint*  
680 *arXiv:2402.12712*, 2024.
- 681 Thomas Unterthiner, Sjoerd van Steenkiste, Karol Kurach, Raphaël Marinier, Marcin Michalski, and  
682 Sylvain Gelly. Towards accurate generative models of video: A new metric & challenges. *CoRR*,  
683 abs/1812.01717, 2018.
- 684 Dani Valevski, Yaniv Leviathan, Moab Arar, and Shlomi Fruchter. Diffusion models are real-time  
685 game engines, 2024. URL <https://arxiv.org/abs/2408.14837>.
- 686 Basile Van Hoorick, Rundi Wu, Ege Ozguroglu, Kyle Sargent, Ruoshi Liu, Pavel Tokmakov, Achal  
687 Dave, Changxi Zheng, and Carl Vondrick. Generative camera dolly: Extreme monocular dynamic  
688 novel view synthesis. *arXiv preprint arXiv:2405.14868*, 2024.
- 689 Vikram Voleti, Chun-Han Yao, Mark Boss, Adam Letts, David Pankratz, Dmitry Tochilkin, Chris-  
690 tian Laforte, Robin Rombach, and Varun Jampani. Sv3d: Novel multi-view synthesis and 3d  
691 generation from a single image using latent video diffusion. *arXiv preprint arXiv:2403.12008*,  
692 2024.
- 693 Jionghao Wang, Ziyu Chen, Jun Ling, Rong Xie, and Li Song. 360-degree panorama generation  
694 from few unregistered nfov images. In *Proceedings of the 31st ACM International Conference on*  
695 *Multimedia*, pp. 6811–6821, 2023.

- 702 Peng Wang and Yichun Shi. Imagedream: Image-prompt multi-view diffusion for 3d generation.  
703 *arXiv preprint arXiv:2312.02201*, 2023.  
704
- 705 Qian Wang, Weiqi Li, Chong Mou, Xinhua Cheng, and Jian Zhang. 360dvd: Controllable panorama  
706 video generation with 360-degree video diffusion model. In *Proceedings of the IEEE/CVF Con-*  
707 *ference on Computer Vision and Pattern Recognition*, pp. 6913–6923, 2024a.
- 708 Weihan Wang, Qingsong Lv, Wenmeng Yu, Wenyi Hong, Ji Qi, Yan Wang, Junhui Ji, Zhuoyi Yang,  
709 Lei Zhao, Xixuan Song, Jiazheng Xu, Bin Xu, Juanzi Li, Yuxiao Dong, Ming Ding, and Jie Tang.  
710 Cogvlm: Visual expert for pretrained language models, 2024b. URL [https://arxiv.org/](https://arxiv.org/abs/2311.03079)  
711 [abs/2311.03079](https://arxiv.org/abs/2311.03079).
- 712 Daniel Watson, Saurabh Saxena, Lala Li, Andrea Tagliasacchi, and David J Fleet. Controlling space  
713 and time with diffusion models. *arXiv preprint arXiv:2407.07860*, 2024.  
714
- 715 Yuqing Wen, Yucheng Zhao, Yingfei Liu, Fan Jia, Yanhui Wang, Chong Luo, Chi Zhang, Tiancai  
716 Wang, Xiaoyan Sun, and Xiangyu Zhang. Panacea: Panoramic and controllable video generation  
717 for autonomous driving. In *Proceedings of the IEEE/CVF Conference on Computer Vision and*  
718 *Pattern Recognition*, pp. 6902–6912, 2024.
- 719 Tianhao Wu, Chuanxia Zheng, and Tat-Jen Cham. Panodiffusion: 360-degree panorama outpanting  
720 via diffusion. In *The Twelfth International Conference on Learning Representations*, 2023.  
721
- 722 Wei Wu, Xi Guo, Weixuan Tang, Tingxuan Huang, Chiyu Wang, Dongyue Chen, and Chenjing  
723 Ding. Drivescape: Towards high-resolution controllable multi-view driving video generation.  
724 *arXiv preprint arXiv:2409.05463*, 2024.
- 725 Shuai Yang, Jing Tan, Mengchen Zhang, Tong Wu, Yixuan Li, Gordon Wetzstein, Ziwei Liu, and  
726 Dahua Lin. Layerpano3d: Layered 3d panorama for hyper-immersive scene generation. *arXiv*  
727 *preprint arXiv:2408.13252*, 2024.  
728
- 729 Hu Ye, Jun Zhang, Sibao Liu, Xiao Han, and Wei Yang. Ip-adapter: Text compatible image prompt  
730 adapter for text-to-image diffusion models. 2023.
- 731 Xiaoding Yuan, Shitao Tang, Kejie Li, Alan Yuille, and Peng Wang. Camfreediff: Camera-free  
732 image to panorama generation with diffusion model. *arXiv preprint arXiv:2407.07174*, 2024.  
733
- 734 Cheng Zhang, Qianyi Wu, Camilo Cruz Gambardella, Xiaoshui Huang, Dinh Phung, Wanli Ouyang,  
735 and Jianfei Cai. Taming stable diffusion for text to 360 {deg} panorama image generation. *arXiv*  
736 *preprint arXiv:2404.07949*, 2024.
- 737 Lvmin Zhang, Anyi Rao, and Maneesh Agrawala. Adding conditional control to text-to-image  
738 diffusion models, 2023.  
739
- 740 Richard Zhang, Phillip Isola, Alexei A Efros, Eli Shechtman, and Oliver Wang. The unreasonable  
741 effectiveness of deep features as a perceptual metric. In *CVPR*, 2018.
- 742 Guosheng Zhao, Xiaofeng Wang, Zheng Zhu, Xinze Chen, Guan Huang, Xiaoyi Bao, and Xingang  
743 Wang. Drivedreamer-2: Llm-enhanced world models for diverse driving video generation. *arXiv*  
744 *preprint arXiv:2403.06845*, 2024.  
745
- 746 Zangwei Zheng, Xiangyu Peng, Tianji Yang, Chenhui Shen, Shenggui Li, Hongxin Liu, Yukun  
747 Zhou, Tianyi Li, and Yang You. Open-sora: Democratizing efficient video production for all,  
748 March 2024. URL <https://github.com/hpcaitech/Open-Sora>.
- 749 Haiyang Zhou, Xinhua Cheng, Wangbo Yu, Yonghong Tian, and Li Yuan. Holodreamer: Holistic  
750 3d panoramic world generation from text descriptions. *arXiv preprint arXiv:2407.15187*, 2024.  
751  
752  
753  
754  
755